

Improving absolute gravity estimates by the L_p -norm approximation of the ballistic trajectory

V D Nagorny

Metromatix, Inc., 111B Baden Pl, Staten Island, NY 10306, USA

E-mail: vn2@member.ams.org

S Svitlov

Institut für Erdmessung, Leibniz Universität Hannover, Schneiderberg 50, D-30167
Hanover, Germany

E-mail: svitlov@ife.uni-hannover.de

A Araya

Earthquake Research Institute, University of Tokyo, 1-1-1, Yayoi, Bunkyo-ku, Tokyo
113-0032, Japan

E-mail: araya@eri.u-tokyo.ac.jp

Abstract. Iteratively Re-weighted Least Squares (IRLS) were used to simulate the L_p -norm approximation of the ballistic trajectory in absolute gravimeters. Two iterations of the IRLS delivered sufficient accuracy of the approximation without a significant bias. The simulations were performed on different samplings and perturbations of the trajectory. For the platykurtic distributions of the perturbations, the L_p -approximation with $3 < p < 4$ was found to yield several times more precise gravity estimates compared to the standard least-squares. The simulation results were confirmed by processing real gravity observations performed at the excessive noise conditions.

Keywords: Absolute gravimeter, L_p -norm approximation, Iteratively Re-weighted Least Squares, antikurtosis

1. Introduction

Absolute ballistic gravimeters measure gravity acceleration by tracking the free motion of the test mass in the gravity field. Having the distances $\{S_1, \dots, S_N\}$ covered by the test mass over the time intervals $\{T_1, \dots, T_N\}$, the acceleration is found as parameter of some trajectory model fitted to the data pairs (T_i, S_i) by methods of the regression analysis. One of the commonly used models describes unperturbed vertical motion of the test mass in the gravity field

$$z_i = z_0 + V_0 T_i + g T_i^2 / 2. \quad (1)$$

The expression (1) represents a linear regression model, because it's defined by a linear combination of the estimated parameters z_0, V_0, g . The estimates are usually found by minimising the sum of the squared discrepancies between the measured data and the model:

$$(z_0, V_0, g) : \sum \epsilon_i^2 \rightarrow \min, \quad \text{where } \epsilon_i = S_i - z_i. \quad (2)$$

Minimised here is the square norm (L_2 -norm) of the vector $\epsilon = \{\epsilon_i\}$, which is a special case of the more general L_p -norm

$$\|\epsilon\|_p = \left(\sum |\epsilon_i|^p \right)^{1/p}, \quad p \geq 1. \quad (3)$$

The tradition of minimising the sum of squares (i.e. finding the *least squares*) has a long and reach history dating back to the beginning of the 19-th century. At that time the main reason for using the least squares was their computational simplicity, as for the $p=2$ the fitting of a linear model is reduced to finding a unique solution for a full-rank system of linear equations. At any other p the equations become non-linear in estimated parameters and require involved computations to find the solution.

Another reason for using the least squares relates to a different kind of linearity: linearity of the estimates with respect to the dependent variable (S_i in our case), which implies no bias of the estimates. Moreover, according to the Gauss-Markov theorem, of all the linear/unbiased estimates, the least-squares deliver the most precise one, in case the errors in the observations are uncorrelated, have zero mean and constant variance. This is especially important in metrology, where the bias may lead to an incorrect estimates of the measurand and its uncertainty.

Nowadays, when advanced computing is no longer a problem, the L_p -approximation with $p \neq 2$ is widely used [1]–[7]. Many researches have noticed that the value of p delivering the lowest variance to the L_p -estimates decreases as the kurtosis[‡] of the error distribution grows; there are formulae suggested for this dependence [8, 9]. Most results have been obtained for the values $1 < p < 2$, that provide better estimates when the noises have heavily-tailed distributions. In trajectory tracking, however, more prevalent are limited-band noises, for which the properties of the L_p -approximation are less known.

The purpose of this work is to investigate the feasibility and possible advantages of approximating the gravimeter's test mass trajectory in different L_p -norms.

The paper has the following structure. The chapter 2 discusses implementation of the Iteratively Re-weighted Least Squares (IRLS) for the L_p -norm approximation. The chapter 3 describes the Monte-Carlo simulation of gravity estimates in L_p -norm. A real-life example of improving the estimates by the L_p -norm approximation is discussed in the chapter 4. We summarise our study in the chapter 5.

[‡] The kurtosis β_2 characterises the spread of the distribution over the possible values of the random variable. It's defined as μ_4/σ^4 , where μ_4 is the fourth central moment, σ is the standard deviation.

2. The L_p -norm approximation by the Iteratively Re-weighted least-squares

We implement the L_p -norm approximation by performing the weighted least-squares (WLS) approximation, in which the weights are defined in a special way [10]. For the model (1), the WLS solution is determined by

$$\boldsymbol{\xi} = \mathbf{A}^+ \mathbf{S}, \quad (4)$$

where

$\boldsymbol{\xi} = (z_0, V_0, g)^T$ is the vector of the unknown parameters,

$\mathbf{S} = (S_1, S_2, \dots, S_N)^T$ is the vector of the observations,

\mathbf{A}^+ is the Moore-Penrose pseudo-inverse matrix calculated as

$$\mathbf{A}^+ = (\mathbf{A}^T \mathbf{V} \mathbf{A})^{-1} \mathbf{A}^T \mathbf{V}, \quad (5)$$

where

$$\mathbf{A} = \begin{pmatrix} 1 & T_1 & T_1^2/2 \\ 1 & T_2 & T_2^2/2 \\ \vdots & \vdots & \vdots \\ 1 & T_N & T_N^2/2 \end{pmatrix} \quad (6)$$

is the experiment design matrix,

$$\mathbf{V} = \text{diag}(v_1, v_2, \dots, v_N) \quad (7)$$

is the diagonal matrix of weights. The approximation in the L_p -norm is achieved when the weights v_i are related to the discrepancies ϵ_i like [10]

$$v_i = |\epsilon_i|^{p-2}. \quad (8)$$

For $p=2$, the weights (8) turn into units, yielding the standard least-squares solution. The formula (8) cannot be used directly to find the weights v_i , because the weights need to be known before the approximation, while the residuals ϵ_i are known only after the approximation is done. Because of that, the WLS is usually applied several times leading to the Iteratively Re-weighted Least Squares. The iterations start with the weights $v_i=1$, i.e. with the regular least-squares. The residuals ϵ_i are then used to build the new weights

$$\mathbf{V} = \text{diag}(|\epsilon_1|^{p-2}, |\epsilon_2|^{p-2}, \dots, |\epsilon_N|^{p-2}), \quad (9)$$

which are then applied to approximate the original data. The iterations can be repeated, but the process is known to sometimes have a problematic convergence. Though different approaches exist to improve the convergence [10], the simulations found that two iterations always produce a sufficiently accurate for our purposes approximation, with the bias not discernible in random noise. For better computational stability we normalised the weights (8), so they would range from 0 to 1:

$$v_i = \left(\frac{|\epsilon_i|}{M} \right)^{p-2}, \quad p \geq 2, \quad (10)$$

where

$$M = \max |\epsilon_i|. \quad (11)$$

If $p < 2$, the powers in (8) become negative, and to prevent zero division errors another modification of the weights was necessary:

$$v_i = \left(\frac{\max(|\epsilon_i|, rM)}{rM} \right)^{p-2}, \quad p < 2, \quad (12)$$

where $r = 0.001$ is a regularisation parameter establishing the threshold of smallness as fraction r of the maximum residual M . According to (12), the residuals below the threshold get replaced with the threshold value rM . A similar way of regularisation is implemented in [7].

3. Modelling the properties of the absolute gravity estimates in the L_p -norm

3.1. Organisation of the simulation experiment

For the simulations, we added random perturbations to the parabolic trajectory (1) with known acceleration $g = 9.8 \text{ ms}^{-2}$ §, and then recovered the acceleration from the perturbed parabola using the L_p -norm approximation (figure 1). The values of p ran from 1 to 6 with the increment of 0.1, so the standard least-squares solution ($p=2$) was also available from the simulation and was used for comparison. To build the parabola, 700 data points $\{T_1, \dots, T_{700}\}$ representing 699 time intervals with the common start at T_1 were used, spanning the total time $T_{700} = 0.22 \text{ s}$. We considered 3 distributions of the T_i -points (experiment designs) found in different types of absolute gravimeters (figure 2). The EST (equally spaced in time) design has the uniform distribution of the T_i -points and is used in both free-fall and rise-and-fall gravimeters. The ESD_{FF} design has the minimal density at the start, linearly increasing towards the end of the interval. The ESD_{RF} design has the minimal density in the centre, linearly increasing towards the start and the end of the interval. These two designs are found in free-fall (FF) and rise-and-fall (RF) gravimeters with the levels equally spaced in distance (ESD). For every type of perturbation we simulated 3000 drops and, after approximating the trajectory in different L_p -norms, analysed the results. Every realisation of the simulated noise was used in all three experiment designs by assigning either EST, ESD_{FF} , or ESD_{RF} realisations of the vector $\mathbf{T} = \{T_1, \dots, T_{700}\}$ to the same noise vector $\boldsymbol{\epsilon} = \{\epsilon_1, \dots, \epsilon_{700}\}$.

The simulations and data analysis were performed with the MATLAB[®] software.

3.2. Simulation results for the random uncorrelated perturbations

The trajectory noise in absolute gravimeters comes from a number of sources, such as ground vibrations, laser stabilisation, digital signal acquisition, fringe counting, etc., so

§ Other parameters were $z_0 = 1 \text{ nm}$ and $V_0 = 0 \text{ ms}^{-1}$. Zero initial velocity was chosen to maximise the difference between the experiment designs.

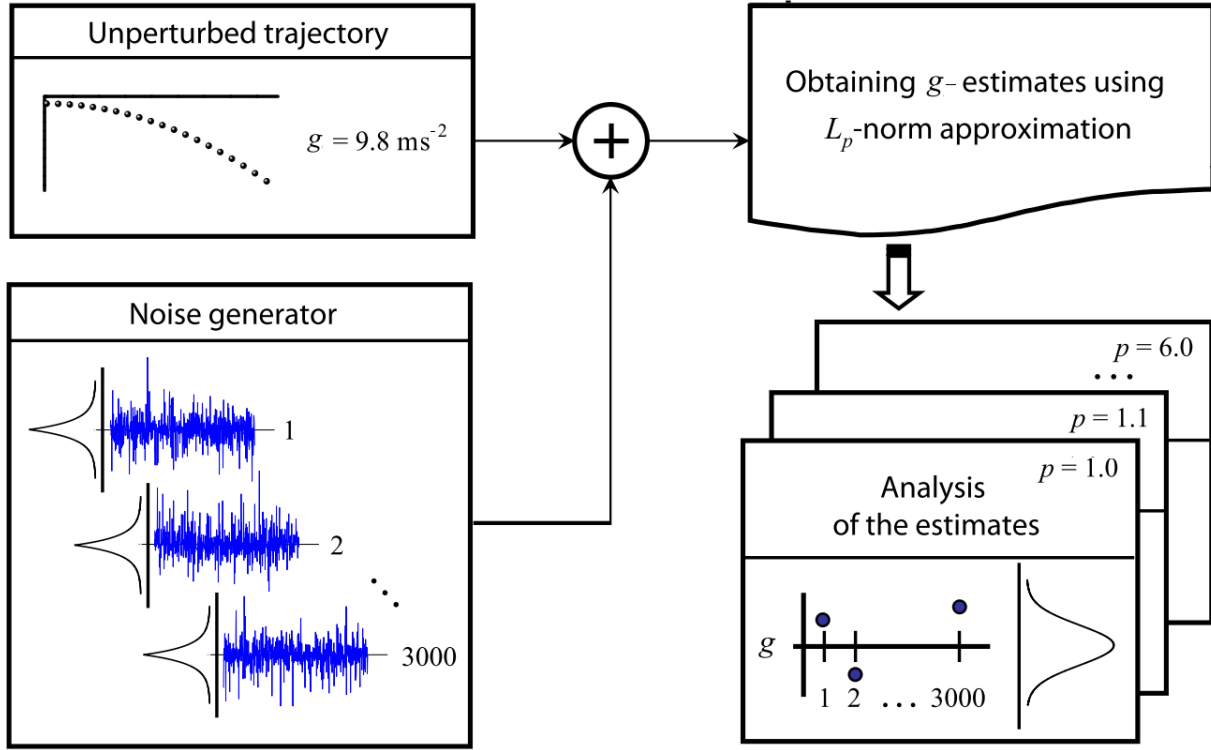


Figure 1. Numerical simulation of the properties of the ballistic trajectory approximation in the L_p -norm.

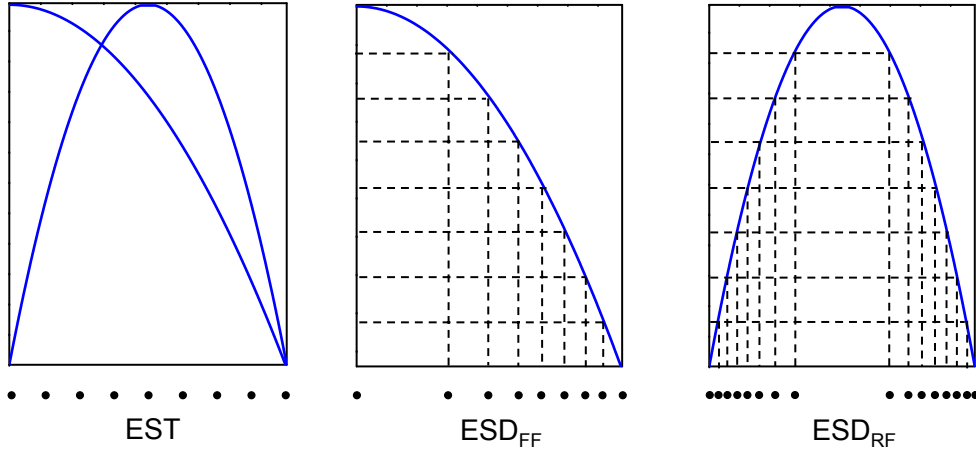


Figure 2. Experiment designs used in the simulation:

EST – equally spaced in time. Time intervals do not depend on the trajectory, can be used in both free-fall and rise-and-fall gravimeters;

ESD_{FF} – equally spaced in distance for the free-fall trajectory;

ESD_{RF} – equally spaced in distance for the rise-and-fall trajectory.

the combined noise most often is of the Gaussian type. Sometimes, however, individual sources can dominate, creating other noise distributions. We did the simulations for several noise types, all having the standard deviation of 1 nm.

For all noise distributions, the distribution of the g -estimates was normal, for any p . For every noise distribution there existed an optimal value of p delivering minimal

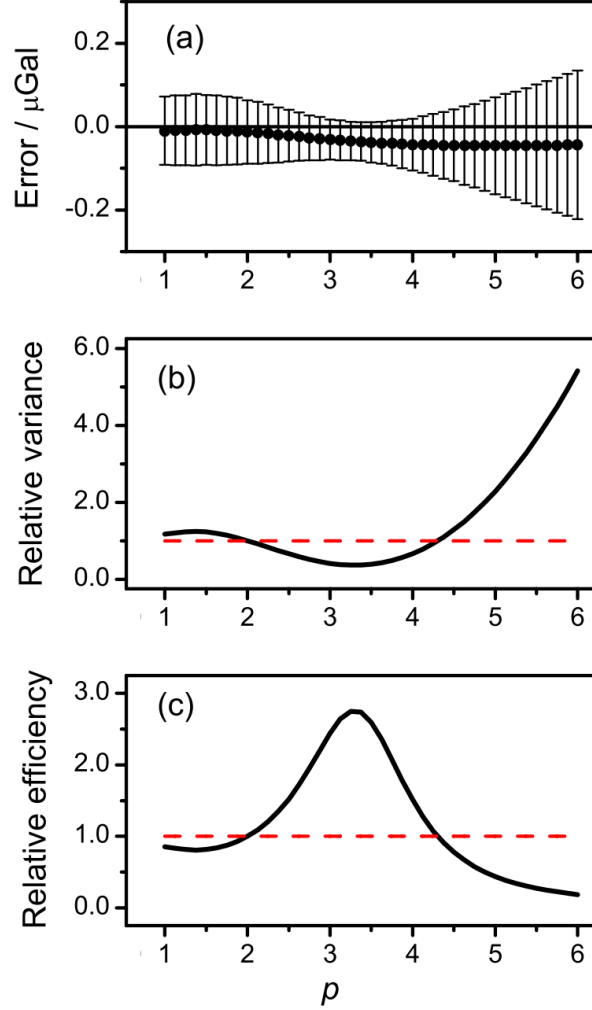


Figure 3. Three ways of graphical representation of the simulation results (noise: Uniform, trajectory sampling: EST)
a – mean gravity estimates shown relatively to the known value of $g = 9.8 \text{ ms}^{-2}$ (1 $\mu\text{Gal} = 10^{-8} \text{ ms}^{-2}$) and their standard deviations as error bars, for different L_p -norms;
b – variance of the L_p -norm estimates relative to the variance of the standard least-squares solution;
c – relative efficiency of the estimates as ratio of the variance of the L_2 -estimate to the variance of the L_p -estimate – shows the number of times the variance has decreased compared to the standard least-squares.

variance of the estimate (figure 3a). The optimal p ranged from 1.4 to 3.3 depending on the noise distribution. This result deviates from the theory [11] predicting no optimal p for at least the Uniform distribution.

For the numeric characteristic of the distribution shape, we used antikurtosis $\|$, because it can only assume values from 0 to 1 for any distribution. We found it more

$\|$ The antikurtosis χ relates to the kurtosis β_2 as $\chi = 1/\sqrt{\beta_2}$ [12].

convenient than the traditionally used kurtosis, which can range from 1 to infinity. The optimal p increased with antikurtosis (table 1), but not always the variance at the optimal p improved substantially. We visualised the improvement by plotting the variance for every p (figure 3b) divided by the variance of the standard least-squares. The factor of the variance improvement is shown on the plot of the inverse ratio (figure 3c), which is equivalent to the relative efficiency of the L_p -estimate compared to the standard least-squares one. The relative efficiency plots for all simulated noises and experiment designs are presented on the figure 4. As seen on the figure and at the table 1, significant improvement of the precision is achieved for the Uniform and Arcsine distributions, if the norm $L_{3.3}$ is used for the parabola fitting instead of the L_2 .

As non-linearity of the L_p -estimates can entail bias, we did the drop-to-drop comparison of the L_2 -estimates (theoretically unbiased) with the L_p -estimates at the optimal p . No statistically significant divergence of the two estimates was detected. We thus confirmed no bias for our approximation procedure, the fact known for the L_p -estimates in case of the symmetric noise distributions [8, 11].

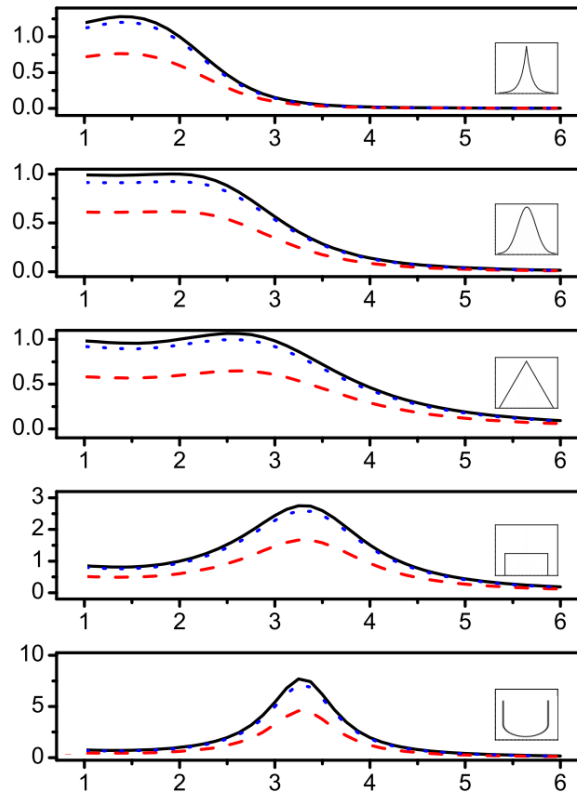


Figure 4. Relative efficiency of the L_p -norm estimates (Y-axis) for different noise types. The efficiency is calculated as ratio of the L_2 -estimate variance for the EST-design to other L_p -estimates for all designs.

— EST, ESD_{RF}, — — — ESD_{FF}.

Table 1. Results of the simulation of the absolute gravity estimates by approximating the trajectory in different L_p - norms. The case of random uncorrelated perturbations of the trajectory.

Noise Distribution	Anti- kurtosis χ	Best p	Rel. eff. ^a for the best p		
			EST	ESD _{FF}	ESD _{RF}
Laplace	0.41	1.4	1.3	1.3	1.3
Normal	0.58	2.0	1.0	1.0	1.0
Triangle	0.65	2.5	1.1	1.1	1.1
Uniform	0.75	3.3	2.8	2.8	2.8
Arcsin	0.82	3.3	7.0	7.0	7.1

^aDetermined as ratio of the variance of the L_2 -estimate to the variance of the L_p -estimate for the same experiment design.

3.3. Simulation results for the “harmonic in the Gaussian noise” perturbations

According to the table 1, the L_p -estimates with $p > 2$ can provide a significant gain in the efficiency when the errors are distributed by the Uniform or Arcsine law. In trajectory tracking such errors are often caused by harmonic perturbations of the reference frame. We modelled the perturbations by the sum of a sinusoid and Gaussian noise. In every simulated drop, a sinusoid with a given frequency f and amplitude of 1.41 nm was assigned an initial phase randomly taken from the uniform distribution on $[0, 2\pi]$, and then sampled according to the experiment design. The sinusoid samples were added by the Gaussian noise, one noise realisation for all three experiment designs. The signal-to-noise ratio (SNR) is defined as quotient of the standard deviations of the sinusoid and the noise, so the infinite SNR means no random noise.

The results of the simulation for the frequencies of 17 Hz, 35 Hz, 55 Hz and the SNR values of ∞ , 100, 10, 2 are shown in the table 2. The antikurtosis χ of the perturbation was from 0.70 to 0.82, typical for the range occupied by the Uniform and Arcsine distributions. The resulting g -estimates have passed the normality test (Lilliefors, 5%) only for some low SNR values. The optimal p and relative efficiencies for which the normality was observed are shaded in the table 2. Like for uncorrelated noises (table 1), there always existed an optimal p delivering the lowest value to the variance of the L_p -estimate. The optimal p was between 2.8 and 3.8, yielding the variance decrease of the estimate between 1.2 and 30.6 times. The values of p and the efficiency gain have a complicated dependence on the signal frequency, the experiment design, and the SNR, so the values have to be evaluated experimentally in every practical case.

4. Example of using the L_p -estimates on real data

The field measurement of absolute gravity are often performed under the harsh geophysical conditions that deteriorate the performance of the instruments. Oftentimes it's not possible to repeat the measurements or improve the conditions, so the

Table 2. Results of the simulation of the absolute gravity estimates by approximating the trajectory in different L_p - norms. The trajectory perturbations are “harmonic in the Gaussian noise.”

f/Hz	SNR	EST			ESD _{FF}			ESD _{RF}		
		χ	p	rel.eff. ^a	χ	p	rel.eff. ^a	χ	p	rel.eff. ^a
17	∞	0.81	3.6	5.5	0.81	3.5	17.5	0.78	3.4	1.5
	100	0.81	3.6	5.8	0.81	3.5	16.9	0.78	3.4	1.5
	10	0.80	3.6	5.5	0.80	3.5	17.7	0.78	3.4	1.6
	2	0.70	3.6	2.7	0.70	3.8	7.4	0.68	3.3	1.2
35	∞	0.82	3.5	29.3	0.82	3.4	22.2	0.82	3.6	14.9
	100	0.82	3.5	29.5	0.82	3.4	23.2	0.82	3.5	15.1
	10	0.81	3.5	22.0	0.81	3.4	19.6	0.81	3.6	13.7
	2	0.70	3.5	2.7	0.70	3.4	3.3	0.70	3.5	3.3
55	∞	0.82	3.3	16.0	0.82	3.3	28.5	0.82	3.3	25.8
	100	0.82	3.3	15.8	0.82	3.3	28.8	0.82	3.3	25.6
	10	0.80	3.3	15.6	0.80	3.3	30.6	0.81	3.3	25.3
	2	0.70	2.8	1.3	0.70	3.1	2.3	0.70	3.1	2.2

^aDetermined as ratio of the variance of the L_2 -estimate to the variance of the L_p -estimate for the same experiment design.

researches have to make the best possible gravity estimates using the available data. As example, we consider a series of measurements taken by the TAG-1 absolute gravimeter developed by the Earthquake Research Institute of the University of Tokyo. The instrument features a laser interferometer with built-in accelerometer for the independent measurement and correction of the ground vibrations, and a homodyne quadrature fringe signal detector [13, 14]. The free-fall trajectory of about 12 cm is sampled with the frequency of 10 MHz (EST-design). A typical drop-to-drop scatter of the g -values at the station ‘Esashi’ is about 20 μGal ¶, so the standard deviation of the mean below 1 μGal is reached in several hundreds drops. The bandwidth of the built-in accelerometer is up to 4 Hz, so the increased intensity of the high-frequency seismic noise could significantly disturb the measurements. The figure 5(a) shows one such noisy set of gravity estimates taken on December 23, 2011 at the ‘Esashi’ gravity station, after applying standard tidal, atmospheric, and polar motion corrections. To obtain the L_p -estimates, the trajectory was decimated to 2 kHz, the standard speed-of-light and gradient corrections were applied to the time and distance coordinates respectively, then the gravity was found using the standard least-squares approximation. The set fails the normality test, making the standard ‘three-sigma’ rejection too restrictive for the obtained heavily-tailed distribution of the L_2 -estimates. However, neither four, nor five sigmas made much difference to the mean g -value or its standard deviation, which remained at about 3 μGal (table 3).

We then approximated the trajectory in the L_p -norm for p ranging from 1 to 6 (see

¶ 1 $\mu\text{Gal} = 10^{-8} \text{ ms}^{-2}$

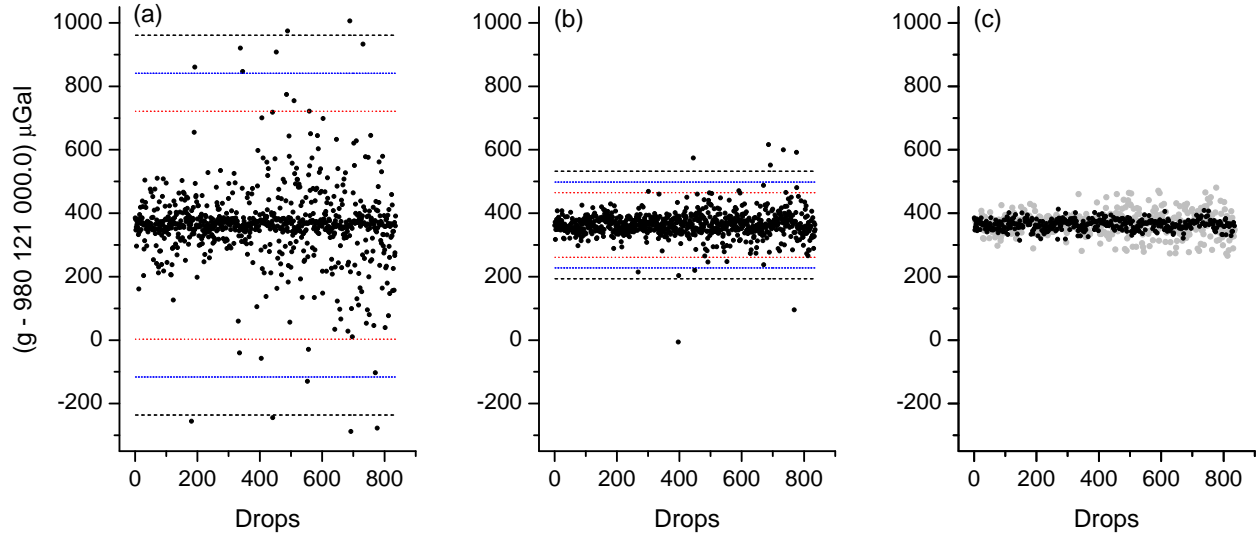


Figure 5. Improving precision of the absolute gravity estimates by using the L_p -norm approximation of the free-fall trajectory:

- (a) standard least-squares approximation ($p=2$), the bars are for the 3σ , 4σ , and 5σ ;
- (b) approximation for $p=3.5$, the bars are for the 3σ , 4σ , and 5σ ;
- (c) mixed $p=2/p=3.5$ approximation based on the antikurtosis of the residuals: black dots – Gaussian group ($p = 2$), grey dots – Arcsine group ($p = 3.5$).

section 2). For each p we obtained the variance of the set gravity estimate and plotted the relevant relative efficiency (figure 6). According to the plot (figure 6(a), curve 1), the variance at $p=3.5$ decreased several times w.r.t. $p=2$, reducing the standard deviation of the mean to about 1 μGal (table 3). Based on the simulations (section 3), the peak of the efficiency at $p > 2$ is suggestive of the residuals with non-Gaussian distributions. We investigated the residuals and found the values of antikurtosis ranging from 0.487 to 0.813, which corresponds to the wide range of distributions – from Laplace to Arcsine (figure 7). The likely reason for the non-Gaussian errors was resonant oscillations of the reference mirror caused by the excessive seismic noise. The most prevalent in the set were residuals with the Gaussian and Arcsine distributions. According to the simulations (section 3), the most efficient L_p -approximations for the Arcsine-noised trajectory were achieved for the values of p between 3 and 4, which explains the decrease of the uncertainty. However, for the Gaussian noises the approximation with p in that range can be several times less efficient than the standard least-squares (figure 4, second from the top). This led us to the idea of splitting the set into two parts with predominantly Gaussian and Arcsine noises, and independent optimising the L_p -norm on each set. We have split the groups at the antikurtosis $\chi = 0.65$, about in the middle of two peaks at the figure 7. Gravity estimates in each group have passed the normality test (Lilliefors, 5%), so further processing was carried out with the 3σ rejection, each group with its own σ . The splitting has increased the efficiency of the estimate for the Arcsine group with $p=3.5$ from 10.0 to 12.5 (figure 6(a), 2). For the Gaussian group we used the

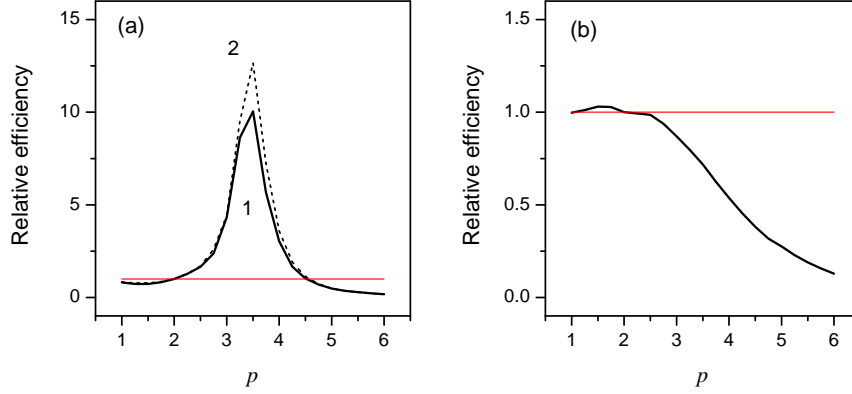


Figure 6. Relative efficiency of the gravity estimates with the L_p -norm approximation of the trajectory:

- (a), 1: The entire set with the 5σ censoring. The variance of the L_p -approximation for $p=3.5$ decreases 10 times.
- (a), 2: The portion of the set with high antikurtosis values. The variance of the L_p -approximation for $p=3.5$ decreases 12.5 times. 3σ censoring applied.
- (b): The Gaussian portion of the set. The standard least-squares ($p = 2$) are close to optimal. 3σ censoring applied.

Table 3. Estimates of the absolute gravity value obtained with different modes of the approximation of the free-fall trajectory

Mode of approximation of the trajectory	Rejection limits	Accepted drops	Set mean \bar{g} / μGal	Set std.dev. $\bar{\sigma}$ / μGal	Mean's std.dev. $\bar{\sigma}$ / μGal
Whole set, L_2	3σ	784	980 121 363.52	80.44	2.87
	4σ	803	980 121 362.38	95.24	3.36
	5σ	811	980 121 363.96	107.31	3.77
Whole set, $L_{3.5}$	3σ	802	980 121 362.70	29.51	1.04
	4σ	817	980 121 363.31	32.67	1.14
	5σ	820	980 121 362.76	33.88	1.18
Split groups, $L_2/L_{3.5}$	$3\sigma/3\sigma$	396/406	980 121 364.50 ^a	16.37/38.18	0.76 ^b

^a Weighted average of two groups, the weights are the reciprocals of the groups' variances

^b Standard deviation of the weighted average

standard least-squares with $p=2.0$, which helped to avoid the decrease of the efficiency at $p=3.5$ for that group (figure 5(b)). Combining the estimates for both groups has reduced the standard deviation of the weighted mean to $0.76 \mu\text{Gal}$ (figure 5(c)). The gravity estimates obtained with different approximations are summarised in the table 3.

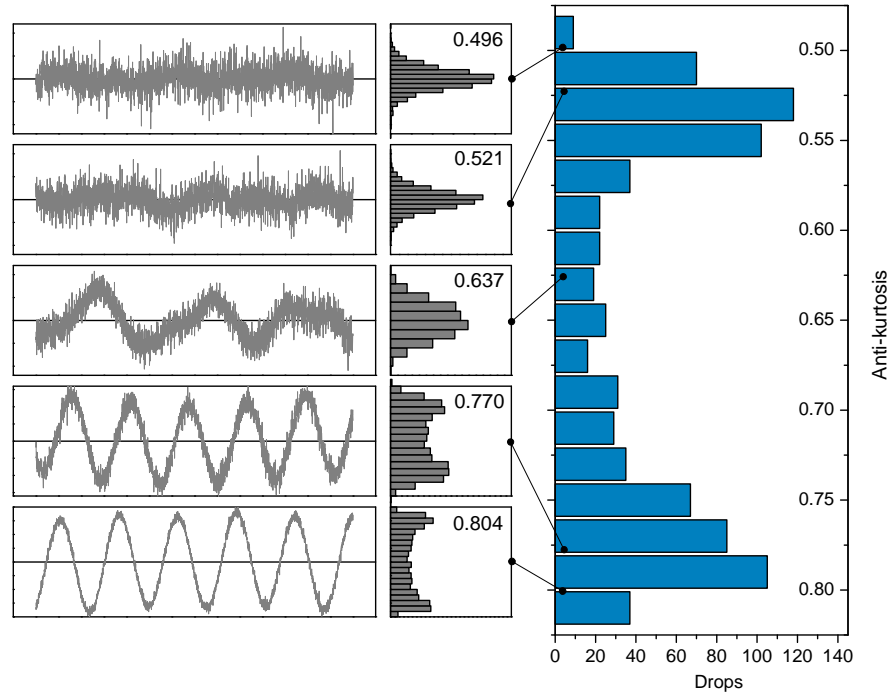


Figure 7. Antikurtosis composition of the noise in the data set.

The histogram on the right-hand side shows the distribution of the antikurtosis for the noises found in the set's drops. The histograms in the middle and the plots on the left-hand side show examples of the noises present in the set. Due to the inclement seismic conditions, the noises cover a wide range of distributions, from Laplace to Arcsine.

5. Conclusions

We have simulated the approximation of the ballistic trajectory in different L_p -norms, in view of using it to improve the absolute gravity estimates. To perform the approximation, the Iteratively Re-weighted Least Squares method was implemented. The estimates were simulated for three different plans of the experiment corresponding to two types of the ballistic trajectory (free-fall, rise-and-fall) and two schemes of data location (equally spaced in time or in distance). Each plan was applied to several perturbation types, including the cases of random uncorrelated noises and a harmonic in the Gaussian noise. As an application example, the simulation results were used to improve the absolute gravity estimates obtained at the 'Esashi' gravity station by the TAG-1 gravimeter.

The following conclusions can be drawn from the study.

- (i) The Iteratively Re-weighted least-squares with two iterations approximate the ballistic trajectory in the L_p -norm with the accuracy sufficient for the purposes of absolute gravimetry. No statistically significant bias of the estimate was found for the wide range of the trajectory noises.
- (ii) The L_p -norm approximation of the ballistic trajectory with $p > 2$ estimates

gravity more precisely than the standard least-squares ($p=2$), if the trajectory perturbations deviate from the Gaussian towards more platykurtic distributions, i.e. those with flattish or concave shape.

- (iii) The observed efficiency maximum for certain values of p on platykurtic distributions disagrees with the prediction of the work [11], where the monotonous increase of the efficiency with the norm power p is obtained for the Uniform distribution. This could possibly be explained by a limited iterations of our IRLS procedure, resulting in a “quasi” rather than the “exact” L_p -approximation.
- (iv) For the same measurement interval T and fixed number of data points N , the EST sampling of the free-fall trajectory makes the gravity estimates about twice as efficient as those with the data equally spaced in distance, for any p . This points to an obvious way of improving the modern free-fall absolute gravimeters, which predominantly use the ESD scheme. For the symmetric rise-and-fall trajectory, the efficiency of the EST and ESD sampling is about the same.

The presented study is a first attempt to obtain the gravity estimates by approximating the ballistic trajectory in the L_p -norm with $p \neq 2$. Many important questions are yet to be answered by future work. The questions include, but are not limited to

- (i) The scope of the applicability of the L_p -norm approximation. For the purposes of absolute gravimetry we investigated only the estimates of the quadratic coefficient of the second-order polynomial model. The results can be applied to other models to build more efficient estimates in wider range of applications.
- (ii) Auto-correlation of the residuals. The main source of the platykurtic distributions is the low-frequency noises. Our simulations of the correlated Arcsine noises and processing of the real data suggest that the efficiency of the L_p -approximation is defined mostly by the noise distribution and is not deteriorated by the auto-correlation of the residuals. Still, the influence of the auto-correlation calls for more thorough investigation, including the comparison to other algorithms of the low-frequency noise filtering.
- (iii) Contaminated distributions within a drop. Further investigations are desirable to better understand the properties of the L_p -norm approximation for the mixed noise distributions, such as harmonics in the Gaussian noise.
- (iv) Contaminated distributions of the set and set splitting. When a set has drops with different noise types, a single value of p may not yield the best L_p -approximations for all drops. In the example (section 4) we have split the set in two at the centre of the antikurtosis histogram. Though we gained certain uncertainty decrease, there may exist better ways of set splitting, worth to be investigated.
- (v) The reasons of the departure of the simulated results from those predicted in [11] have to be investigated to better understand the properties of the IRLS algorithm of the L_p -approximation.

References

- [1] F Pennecchi, L Callegaro, “Between the mean and the median: the L_p estimator,” *Metrologia*, vol. 43, p. 213, 2006.
- [2] R Willink, “On the L_p estimation of a quantity from a set of observations,” *Metrologia*, vol. 44, p. 105, 2007.
- [3] C Marx, “On resistant L_p -norm estimation by means of iteratively re-weighted least-squares,” *J. Appl. Geodesy*, vol. 7, p. 1, 2013.
- [4] Jeng-Ming Chen; Chen, Bor-Sen, “System parameter estimation with input/output noisy data and missing measurements,” *Signal Processing, IEEE Transactions on*, vol.48, no.6, pp.1548 – 1558, 2000.
- [5] Walach, E. and Widrow, B. “The least mean fourth (LMF) adaptive algorithm and its family,” *Information Theory, IEEE Transactions on*, vol.30, n.2, p.275-283, 1984
- [6] Gui G., and Adachi F., “Sparse least mean fourth algorithm for adaptive channel estimation in low signal-to-noise ratio region,” *Int. J. Commun. Syst.*, vol. 27, 3147–3157, 2014.
- [7] Scales, J. A. and Gersztenkorn, A., “Robust methods in inverse theory,” *Inverse Problems*, vol. 4, p. 71, 1988.
- [8] A. H. Money, J. F. Affleck-Graves, M. L. Hart, G. D. I. Barr “The linear regression model: L_p norm estimation and the choice of p ,” *Communications in Statistics - Simulation and Computation*, vol. 11, Iss.1, p.89-109, 1982.
- [9] V. A. Sposito, M. L. Hand, B. Skarpness “On the efficiency of using the sample kurtosis in selecting optimal L_p estimators,” *Communications in Statistics - Simulation and Computation*, vol. 12, Iss.3, p.265-272, 1983.
- [10] C. Burrus, “Iterative Re-weighted least-squares,” *OpenStax-CNX Web site*. <http://cnx.org/content/m45285/1.12/>, Dec 17, 2012.
- [11] H. Nyquist “The optimal L_p norm estimator in linear regression models,” *Communications in Statistics - Theory and Methods*, vol. 12, Iss.21, p.2511-2524, 1983.
- [12] Novitskiy, P.V.; Zograf, I.A. “Estimation of Errors of Measurements Results.” Leningrad: Energoatomizdat, 1991, 304 p. [in Russian].
- [13] A. Araya, H. Sakai, Y. Tamura, T. Tsubokawa, and S. Svitlov, “Development of a compact absolute gravimeter with a built-in accelerometer and a silent drop mechanism”, *Proc. of the International Association of Geodesy (IAG) Symposium on Terrestrial Gravimetry: Static and Mobile Measurements (TGSM-2013)*, 17-20 September 2013, Saint Petersburg, Russia, p.98, 2014.
- [14] S. Svitlov and A. Araya, “Homodyne interferometry with quadrature fringe detection for absolute gravimeter,” *Appl. Opt.* vol. 53, p. 3548, 2014.